The Application of Micro- and Nano-Sized Zinc Oxide Particles Differently Triggers Seed Germination in Ocimum basilicum L., Lactuca sativa L., and Lepidium sativum L. under

horticulturae

MDPI

Article

The Application of Micro- and Nano-Sized Zinc Oxide Particles Differently Triggers Seed Germination in *Ocimum basilicum* L., *Lactuca sativa* L., and *Lepidium sativum* L. under Controlled Conditions

Matteo Caser [1,*], Nicolò Maria Percivalle [2] and Valentina Cauda [2]

[1] Department of Agricultural, Forest and Food Sciences, University of Torino, Largo Paolo Braccini 2, 10095 Grugliasco, TO, Italy
[2] Department of Applied Science and Technology, Politecnico di Torino, Corso Duca Degli Abruzzi 24, 10129 Turin, TO, Italy; nicolo.percivalle@polito.it (N.M.P.); valentina.cauda@polito.it (V.C.)
* Correspondence: matteo.caser@unito.it

Abstract: Zinc oxide (ZnO) particles have recently received attention in different agriculture sectors as new technologies and practices are entering into force with limited adverse effects on the environment. However, various works have reported both positive or negative effects on plants. The present study focused on an evaluation of the effects of four different new micro- and nano-sized ZnO particles (namely, Desert Roses (DRs), MultiPods (MPs), NanoFlakes (NFs), and NanoParticles (NPs)) on the seed germination traits of *Ocimum basilicum* L., *Lactuca sativa* L., and *Lepidium sativum* L. ZnO particles were applied at concentrations of 12.5 ppm, 25 ppm, and 50 ppm. Seeds moistened with deionized water were used as a control. All the particles were characterized by field emission scanning electron microscopy, and their production of Reactive Oxygen Species (ROS) under seed germination conditions was evaluated through electron paramagnetic resonance spectroscopy. Seeds of each species were put on filter paper under controlled conditions in both dark and light photoperiods. In this bioassay, the final germination percentage (FGP), early root length, and index of germination were evaluated. The results showed a wide variability of response to the type and concentration of ZnO particles and to the applied photoperiod of the three studied species. *O. basilicum* FGP increased when treated with NPs and DRs already at the lowest concentration and especially in light conditions with values significantly superior to those of the control (71.1%, 69.4%, and 52.2%, respectively). At higher concentrations, phytotoxicity on root length was observed, with a reduction of circa 30% in comparison to untreated seeds. On the contrary, in *L. sativum*, a phytotoxic effect was seen in radicle length with all the used ZnO particles and concentrations. *L. sativa* seeds did not show significant effects due to the type of particles, with a reduction in FGP only at higher concentrations and particularly in light conditions. Upon light irradiation, different levels of ROS were counted by the application of ZnO particles. DRs produced the highest amount of DMPO-OH adduct (up to 2.7×10^{-5} M) followed by the NP type (2.0×10^{-5} M). Taking together all these findings, the seeds' coat morphology, their ability to absorb ZnO particles, and the ROS production in light conditions are indeed crucial players in the application of these formulations in seed germination.

Keywords: ZnO particles; ROS production; germination index; horticulture

Citation: Caser, M.; Percivalle, N.M.; Cauda, V. The Application of Micro- and Nano-Sized Zinc Oxide Particles Differently Triggers Seed Germination in *Ocimum basilicum* L., *Lactuca sativa* L., and *Lepidium sativum* L. under Controlled Conditions. *Horticulturae* **2024**, *10*, 575. https://doi.org/10.3390/horticulturae10060575

Received: 5 April 2024
Revised: 1 May 2024
Accepted: 23 May 2024
Published: 31 May 2024

1. Introduction

Seed germination is one of the most crucial and complex biochemical and physiological phenomena in the plant lifecycle [1]. Effective seed germination is the key to better crop development and yield and several efforts are being made to ensure high and synchronized seed germination rates. Among different seed-stimulating methods, priming is an approach to enhancing seed quality, yield, and environmental stress tolerance [2,3]. This method

consists of seed exposure to an eliciting factor that triggers the pre-germinative metabolism and consequently enhances the final germination rate and the seedling emergence, resulting in greater survival under adverse environmental conditions [2]. The most used priming methods are hydropriming, osmopriming, hormonal priming, nutrient priming, and nanopriming [4,5].

Sustainability in agriculture mainly depends on the development of new technologies and practices with limited negative effects on the environment while still improving food quality and yield [6]. In recent years, the use of functionalized nanoparticles has received much attention due to their positive effects on different agriculture aspects [7]. In fact, nanoparticles can contain herbicides, pesticides, fertilizers, or even genes, moving into plant cell organs and releasing their contents [8–10]. A recent application of nanoparticles is nanopriming. Due to their specific characteristics of smaller size (ranging between 1 nm and 100 nm), large surface area, and slow rate of release, nanoparticles can be absorbed by seeds and activate the metabolism [11], thus resulting in a higher seed germination rate and uniformity, such as in *Oryza sativa* L., *Lupinus termis* L., *Triticum aestivum* L., *Zea mays* L., and *Vigna radiata* (L.) R. Wilczek [12–19]. As seed priming agents, different metals, metal oxide nanoparticles, and carbon-based nanoparticles have been applied to enhance germination [20]. Among them, zinc oxide nanoparticles (ZnO-NPs) have received much attention in agriculture due to their unique and desirable properties. ZnO is an n-type semiconducting metal oxide [21] that is widely used in many different fields as well as a nano-priming agent [22]. Depending on the synthesis conditions, it can be easily prepared as micro- or nano-sized particles [23] with different shapes promoting a large specific surface area. In general, it is considered a safe material (being approved by the FDA and EMA in its micrometer form) with low toxicity and the capacity to dissolve into zinc (Zn^{2+}) cations [24]. ZnO nanoparticles are known to generate Reactive Oxygen Species (ROS) under light excitation [25]. At the organism level, high concentrations of ROS are involved in cell signaling and complex morphological, physiological, and biochemical modifications such as autophagy and programmed cell death [26,27]. Peng et al. [28] reported that the aggregation and dissolution of NPs and ROS generation by NPs can be influenced by many factors, including the size, shape, and surface charge of NPs. However, very limited information about the effect of ROS induced by ZnO particles on seed germination is available in the literature. At the biological level, zinc is one of the major essential micronutrients required for seed germination, plant growth, enzyme activity, chlorophyll production, pollen function, and fertilization [29,30]. Recent findings suggest that the utilization of zinc oxide nanoparticles entails both advantages and drawbacks, contingent upon factors such as concentration, synthesis technique, and the subject under examination. Previous research has showcased the potential of ZnO NPs in enhancing seed germination, promoting plant growth, and mitigating diseases due to their antimicrobial properties. The varied impacts of ZnO NPs on plant growth and metabolism during different developmental stages have been well documented, encompassing both favorable and adverse effects [31]. Understanding the behavior of nanoparticles (NPs) necessitates consideration of various factors such as particle size, size distribution, shape, surface and core chemistry, crystallinity, agglomeration state, purity, redox potential, catalytic activity, surface charge, and porosity [31]. In in vitro conditions, nano-sized ZnO particles (20 nm) increased the root length and aerial biomass of *V. radiata* and *Cicer arietinum* L. at the concentrations of 1.0 and 20.0 mg L^{-1}, respectively [32]. However, for different plants, different concentrations and forms of ZnO NPs can be toxic. This is because NPs can accumulate in plant tissues, which can affect physiological and biochemical processes. The literature suggests that ZnO NPs can inhibit different developmental stages [33], reducing plant biomass and yield [34]. For example, [34,35] reported that concentrations of ZnO NPs higher than 50 mg L^{-1} in hydroponic cultivation limited root elongation in *Lolium perenne* L., *Raphanus sativus* L, and *Brassica napus* L.

Regarding seed germination, Lin and Xing [34] and Lee et al. [36] reported that an inhibition was observed by using ZnO NPs at concentrations ranging from 2000 to

4000 mg L^{-1} in *L. perenne* and *Fagopyrum esculentum* Moench, respectively, while an increase in the seed germination and root elongation of *R. sativus* and *B. napus* was obtained at lower contents (2 mg L^{-1}) [34]. Similar results were also obtained with much higher concentrations (600 mg L^{-1} and 1000 mg L^{-1}) in seeds of *Vigna mungo* (L.) Hepper and *Arachis hypogaea* L. [37,38]. Priming seeds with ZnO nanoparticles resulted in increased Zn content in the primed seeds, thus contributing to better seedling growth and yield [22].

However, only a limited number of studies on the effects of different ZnO NPs as primers for seed germination in the horticultural sector are available [39], although a relatively broad range of species have been tested. Moreover, the response of plants to the presence and infiltration of ZnO nanoparticles depends on many factors such as type, size, concentration, duration of exposure, and plant type [40,41].

Horticultural crops face ongoing challenges from both severe biotic and abiotic stresses, resulting in diverse impacts that contribute to global food scarcity. Therefore, achieving a balance between horticultural yield and food demand requires the implementation of strategies to help plants adapt to stressful conditions. Thus, in the present work, for the first time, four different ZnO nano- and microparticles with various morphologies and sizes were tested and compared to evaluate their effect on the germination traits of three species for horticultural purposes: *Ocimum basilicum* L., *Lactuca sativa* L., and *Lepidium sativum* L. These species were used because they represent the main models of horticultural plants for evaluating germination performances. The aim of this work was to unravel the role of nano- and microparticles, specifically of ZnO, as primers for seed germination. Secondary objectives concerned the possible effects on priming seeds made by different ZnO sizes, morphologies, and concentrations, as well as their ability to generate ROS under culture conditions.

2. Materials and Methods

2.1. Synthesis and Characterization of ZnO Micro- and NanoParticles

Both micro-sized and nano-sized particles were synthesized and used in this work. The synthesis of ZnO particles was carried out following a sol–gel method, as previously reported by Lops et al. [23], which enabled us to produce different ZnO morphologies, i.e., Desert Roses (DRs), Multipods (MPs), and Nanoflakes (NFs), depending on the amount of base used. The synthesis precursor, zinc nitrate hexahydtrate ($Zn(NO_3)_2 \cdot 6H_2O$ 99%, Merck KGaA, Darmstadt, Germany, 7.4 g, 0.0249 mol), was dissolved in 50 mL of double-distilled water, while the base, potassium hydroxide (KOH, 85%, Merck KGaA, Darmstadt, Germany), was prepared by dissolving different amounts in 50 mL of double-distilled water in a Teflon vessel. In particular, 2.794 g (0.0498 mol), 11.177 g (0.1992 mol), and 16.766 g (0.2988 mol) of KOH were prepared to obtain DRs, MPs, and NFs, respectively. The zinc nitrate solution was dropwise added to the respective KOH solution under vigorous stirring, obtaining a final solution of 100 mL, with a molar ratio between the base and the Zinc precursor of 2 for DRs, 8 for MPs, and 12 for NFs. The obtained gels were then closed by a screw cap in the Teflon reactors and aged in an oven at a mild temperature (70 °C) for 4 h. At the end of the reaction, the ZnO microparticles were deposited as white powders at the bottom of the reactor and separated from the water solution by filtration. The powders were thoroughly washed with deionized water until the pH of the washing solution turned to neutral values. Finally, the three produced microparticles were dried in air at 60 °C overnight to obtain a powder form and then dispersed in double-distilled water at a 1 mg mL^{-1} concentration for further experiments, described in Section 2.2.

The synthesis of ZnO nanocrystals (NCs) was carried out by microwave-assisted solvothermal synthesis, as previously reported [42]. Zinc acetate di-hydrate ($Zn(CH_3COO)_2 \cdot 2H_2O$ Puriss. P.a., 99%, Merck KGaA, Darmstadt, Germany) as a zinc precursor was dissolved in methanol (0.09 M, 60 mL) under stirring in a Teflon reactor vessel, equipped with pressure and temperature probes for microwave furnace reaction. To promote zinc oxide nucleation, 480 µL of double-distilled water was added and then a potassium hydroxide (KOH, 85% pellets, Merck) solution in methanol (0.2 M, 35 mL) was added to the reactor vessel and

inserted into the microwave furnace (Milestone START-Synth, Milestone Inc., Shelton, CT, USA) for 30 min at 60 °C. The resulting colloidal suspension was then processed by centrifugation with two washing steps in ethanol (99%, Merck), each for 10 min at 3500× *g* (Mega Star 600R, VWR International Srl, Milan, Italy). Finally, the pelleted nanoparticles were dispersed in 15 mL of fresh ethanol through sonication (LABSONIC LBS2, FALC Instruments Srl, Treviglio (BG), Italy). A given amount of suspension was then centrifuged again and the ethanol was removed and replaced with double-distilled water to obtain a 1 mg mL^{-1} concentrated stock for further experiments described in Section 2.2.

The characterization of the four ZnO particles (DRs, MPs, NFs, and NCs) was performed by field emission scanning electron microscopy (FESEM, Merlin, ZEISS, Jena, Germany) operated at 5 kV with an in-lens detector to evaluate morphology and size. The crystalline nature was verified by X-ray diffraction (XRD) on a Panalytical X'Pert diffractometer in θ–2θ Bragg-Brentano configuration equipped with a source of radiation Cu-K (λ = 1.54 Å, 40 kV, and 30 mA). For both measurements, 100 µL of the water suspension of micro- and nanoparticles was dried on a silicon wafer and mounted on the sample holder of the respective instruments. To evaluate the photoluminescence properties of ZnO particles, UV–Vis spectrophotometry was employed to record absorbance spectra (in water suspension at a concentration of 0.5 mg mL^{-1}) using a Multiskan GO microplate UV–Vis spectrophotometer (Thermofisher Scientific, Waltham, MA, USA) in a 96-well quartz glass plate (Hellma). For all spectra, the background was subtracted. Furthermore, all particles were analyzed using a wide-field fluorescence inverted microscope (Eclipse Ti-E, Nikon Metrology Europe NV) equipped with a super bright wide-spectrum source (Shutter Lambda XL, Nikon), a high-resolution camera (Zyla 4.2 Plus, 4098 × 3264 pixels, Andor Technology Ltd., Belfast, UK), and an immersion oil 100× objective (Nikon). The particles, dispersed in water at a concentration of 0.1 mg mL^{-1}, were spotted on a glass slide, coated with a cover glass slip, and then sealed with nail polish. The samples were imaged after excitation using different filters at 340 nm and 490 nm and in bright field. The collected images were analyzed with the NIS-Element software Vers. 4.50.

2.2. Plant Material and ZnO Particle Treatment

The seed germination test was evaluated at the Dept. of Agricultural, Forest and Food Sciences (DISAFA) laboratory of the University of Torino (Italy) through in vitro seed germination tests. Seeds of *O. basilicum* 'Superbo' were provided by RB Seeds (Torino, Italy), while *L. sativa* 'White Boston' and *L. sativum* 'Inglese' were provided by Fratelli Ingegnoli Spa (Milano, Italy). Starting from the stock water suspensions of ZnO NPs at 1 mg mL^{-1}, dilutions of the particles with deionized water were performed to obtain solutions containing 12.5, 25.0, and 50.0 mg L^{-1} for each ZnO particle type. For seed priming, different concentrations of ZnO NPs were freshly prepared by dispersing the particles in deionized water using ultrasonic vibration (100 w, 40 kHz) for 30 min.

2.3. Seed Germination Test

Based on the International Rules for Seed Testing Association (2014) [43], seed germination at 23 °C was performed applying two different photoperiod conditions (light/dark at 0/24 h or 24 h/24 h; 500 µmol m^{-2} s^{-1}). One hundred seeds were used for each species per treatment (10 repetitions by 10 seeds). Seeds were placed to germinate in 9 cm lidded Petri dishes containing Whatman No. 1 filter paper and treated with 5 mL of each type and concentration of ZnO NP. Seeds moistened with 5 mL of deionized water were used as a control. Seeds were considered germinated when seedling structures (emergence of the radicle at the peduncle end of the seed) were visible. Non-germinated seeds were classified as dead or vane. The trial was repeated three times. After 72 h, the final germination percentage (FGP), root length, and index of germination (IGe%) were calculated as follows, according to Caser et al. [44,45]:

$$IGe\% = (ns \times rs/nc \times rc) \times 100 \quad (1)$$

where n is the number of germinated seeds and r is the mean root length of the treated sample (s) and the control (c).

2.4. Reactive Oxygen Species Content Evaluation Water Dissolution Test

The possible production of free radicals, i.e., Reactive Oxygen Species (ROS), and, in particular, the most abundant hydroxyl (·OH) radical generated by ZnO particle illumination under seed germination conditions were evaluated through Electron Paramagnetic Resonance (EPR) spectroscopy. In detail, an EMXNanoX-Band spectrometer (Bruker, Billerica, MA, USA) assisted by a spin-trap molecule (dimethylpirrolidone—DMPO from Merck) was used. The ZnO particle suspensions were prepared at 0.5 mg mL^{-1} in water (a higher concentration than in the germination experiments) for ease of detection under EPR; then, the DMPO was added (10 mM) and the suspensions were exposed to either dark conditions or the same illumination conditions used for the seed germination tests (500 µmol m^{-2} s^1 or 840 PPFD corresponding to 395 W m^{-2} for 10 min). The solution was then inserted into the instrument and the EPR spectra were recorded using the following measurement conditions: center field 3428 G, sweep time 60.0 s, sample g-factor 2.00000, number of scans 10. The spectra analysis was then run using the Bruker SpinFit software.

2.5. Water Dissolution Test

Water dissolution tests on ZnO particles were conducted by diluting the ZnO stock suspensions (1 mg mL^{-1}) down to 12.5, 25.0, and 50.0 mg L^{-1} for each ZnO particle type and 5 mL of these dilutions was prepared, each one in triplicate, in plastic (PP) vials. The solutions were then stored in dark conditions for 72 h at room temperature. After this time, the vials containing each ZnO sample were centrifuged at 5000× *g* for 10 min and the supernatants were further filtered with syringe filters of 0.1 µm cut-off (Whatmann, Merck). Finally, the supernatants, which were supposed to contain zinc cations as a result of ZnO particle dissolution, were analyzed through Graphite Furnace Atomic Absorption Spectroscopy (GF-AAS). The Zn content was determined for each solution following the EPA method 289.1.

2.6. Statistical Analysis

Arcsin transformation was performed on all percent incidence data before statistical analysis in order to improve the normality (Shapiro–Wilk test, $p \geq 0.05$) and homoscedasticity (Levene test, $p \geq 0.05$) of data. For all parameters, mean differences were computed using a one-way and univariate ANOVA with the Tukey post-hoc test ($p \leq 0.05$) and pairwise comparisons were performed using Student's *t*-test. All analyses were performed with SPSS 26.0 Inc. software (Chicago, IL, USA).

3. Results

3.1. ZnO Micro and Nanoparticle Traits

The FESEM images were recorded on the four different ZnO samples. As reported in Figure 1, the adopted synthesis routes allowed us to obtain two types of micro-sized particles showing nanometric features at their surface (Figure 1A,B) and two different nano-sized particles (Figure 1C,D). In more detail, Desert Rose (DR) morphology was obtained, with an overall round-shaped structure of 2 µm in diameter composed of nanostructured flakes 15 nm in thickness (Figure 1A). The obtained MultiPods (MPs in Figure 1B) also had a generally round shape and were composed of a multitude of protruding microwires of 2–3 µm in length and 100 nm in lateral size each. They showed a hexagonal cross-section and a pencil-like end shape. The third obtained structure (reported in Figure 1C) was an aggregate of NanoFlakes (NFs) of different sizes varying from 100 nm to 300 nm and with a thickness of 15 to 30 nm each. Finally, the NanoCrystals (NCs) in Figure 1D had an overall spherical shape of 30 nm in diameter with a hexagonal cross-section in most cases.

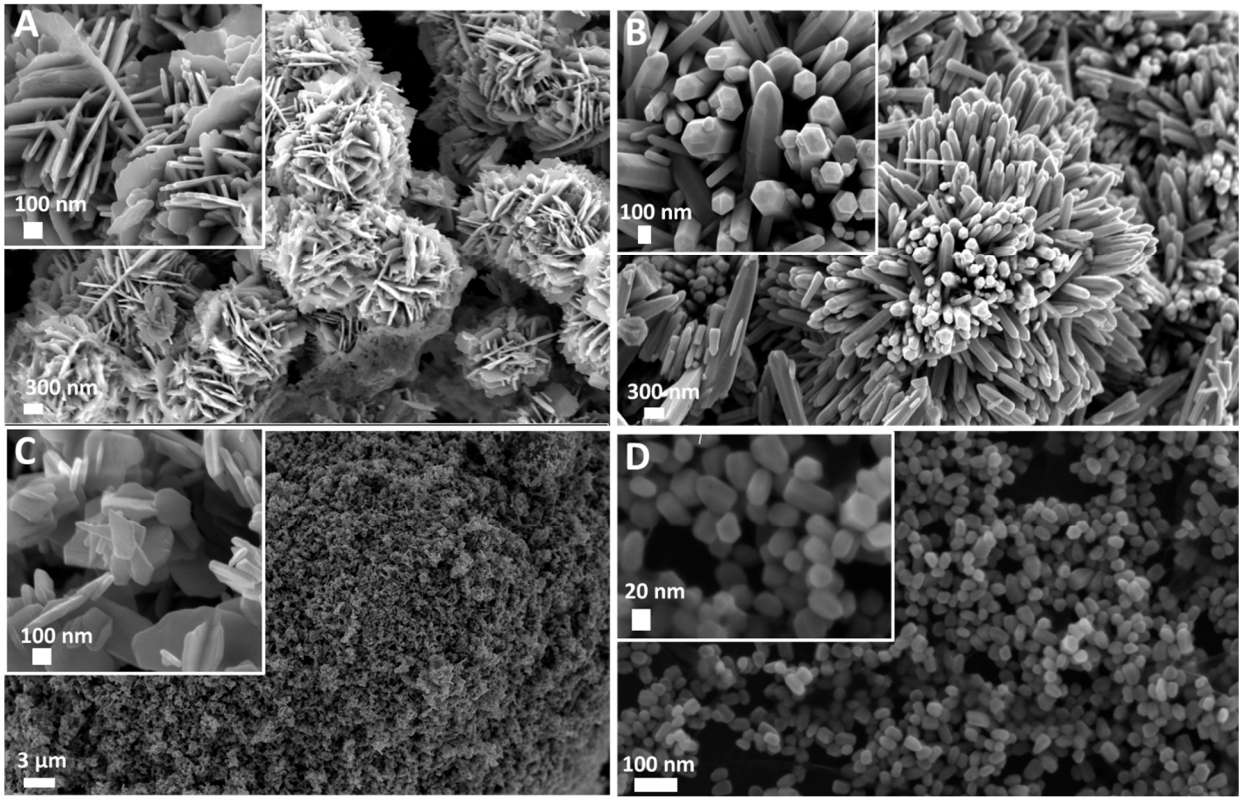

Figure 1. Field Emission Scanning Electron Microscopy (FESEM) images of ZnO micro and nanoparticles used for the seed germination tests. (**A**) Desert Roses (DRs); (**B**) MultiPods (MPs); (**C**) NanoFlakes (NFs); (**D**) NanoCrystals (NCs).

X-ray diffractograms (Figure 2) showed that all ZnO particles were crystalline, with the typical diffraction peaks belonging to the wurtzitic phase (hexagonal, space group P63mc), assigned with Miller indexes according to the JCPDS 80-0074 card. All diffraction peaks were sharp, indicating that the ZnO powders had a high degree of crystallinity and high purity. The differences in diffraction spectra among the micro-sized particles (Figure 2A) and the nano-sized ones (Figure 2B) were due to the particle sizes and their average crystallite sizes.

The possible effects of the incident light on the ZnO particles were examined by different methods: firstly, UV–Vis scanning spectroscopy was conducted to understand the absorption spectra of the different ZnO particles. As expected, all the ZnO particles adsorbed light in the UV range of 200 to 400 nm (Figure 3A). Their optical band gap (Eg) was determined by adopting the Tauc method (Figure 3B) calculated from the absorption spectra. The Eg of the ZnO samples was in the range between 3.1 and 3.3 eV, confirming that all ZnO structures had a broad band gap and semiconductor behavior, allowing their photoexcitation by light with energies in the UV range, as also present in the solar spectrum.

The photoluminescence of the four ZnO particles was recorded by exciting them with different wavelengths in the UV range, i.e., at 340 and 480 nm, and visualizing their possible emission in the blue (430–480 nm) and green (510–550 nm) channels of a fluorescence microscope. The results are reported in the Supporting Information (S.I.), Figures S1–S4. The data show that all the ZnO particles, except the NFs, upon UV excitation, could emit light in both the blue and green channels. This confirmed moderate photoluminescence of the microparticles, i.e., DRs, MPs, and NCs, and, as a whole, the capability of these ZnO particles to be photoexcited by UV light and re-emit it at a higher wavelength (i.e., at lower energy).

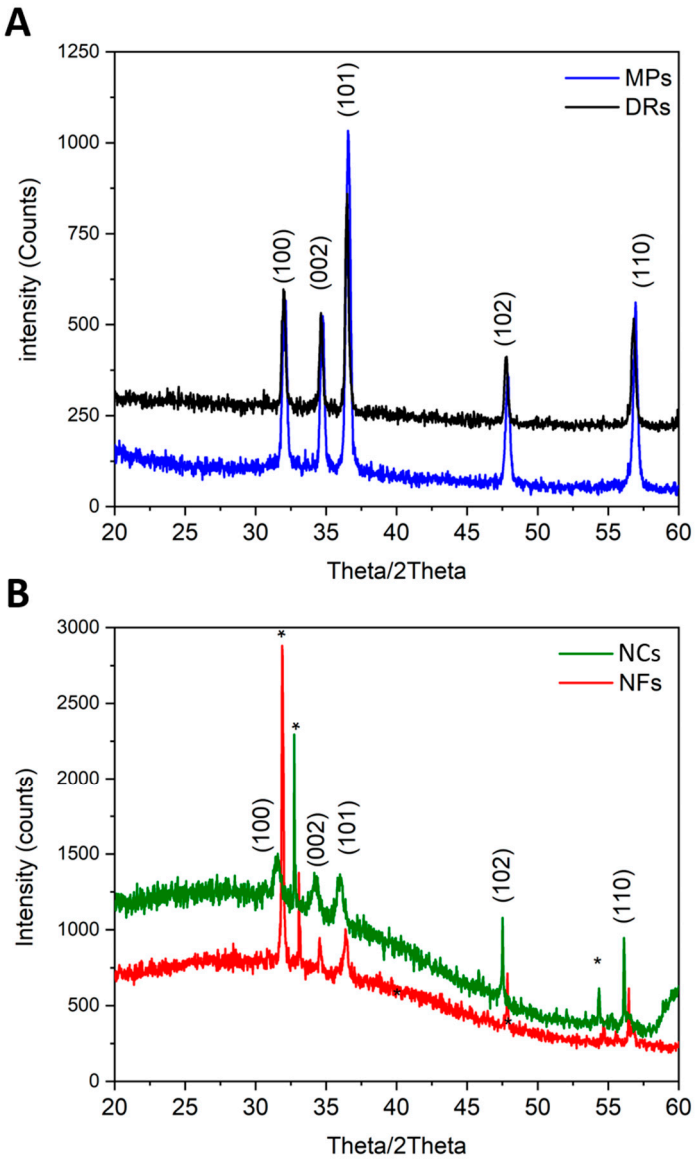

Figure 2. X-ray diffraction patterns of (**A**) micro-sized particles, i.e., DRs and MPs, and (**B**) nano-sized particles, i.e., NCs and NFs. The diffraction peaks are indexes with Miller indexes according to the wurtzite structure of ZnO. Asterisks * refer to the underlying silicon wafer substrate.

3.2. Effect of ZnO Particles on Seed Germination Traits of O. basilicum, L. sativa, and L. sativum

Among the tested ZnO particles, NCs and DRs increased the FGP of *O. basilicum* seeds, with values significantly superior to those of the control (71.1%, 69.4%, and 52.2%, respectively) (Table 1). DRs also resulted in superior Ige% to the control (+41.4%), while no effect on radicle length was observed. All the tested dosages were effective in enhancing FGP in comparison to the control treatment, while a significant reduction in radicle length was observed with the application of the highest concentration in comparison to the lowest (3.86 cm and 5.35 cm in 50.0 mg L^{-1} and 12.5 mg L^{-1}, respectively). No effect of the two applied photoperiods on the studied traits was observed between control treatments (Table 2). Thus, the presence of the light (photoperiod of 24 h/24 h) was effective in increasing all the parameters (~+11% in FGP, ~+37% in radicle length, and ~+ 80% in Ige, respectively).

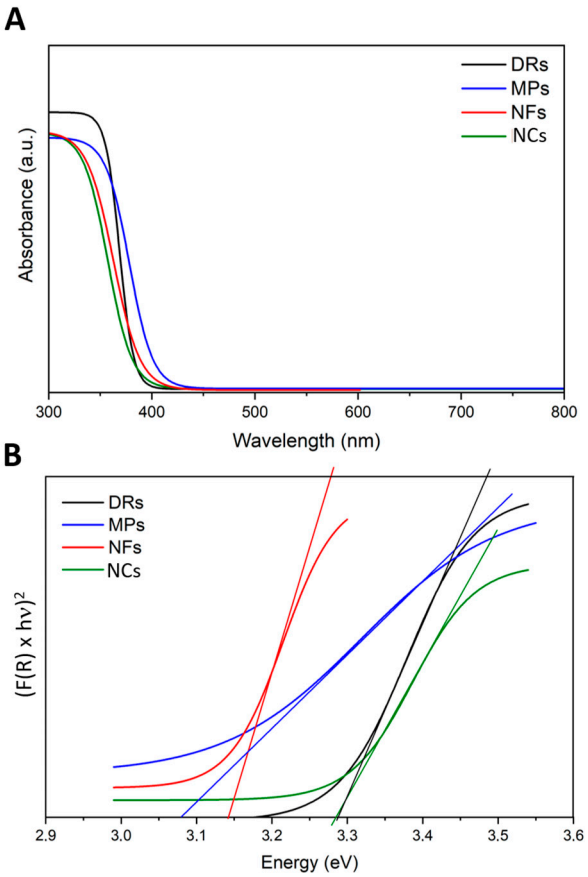

Figure 3. (**A**) UV-visible absorption spectra and (**B**) Tauc plots related to the four ZnO particle morphologies: Desert Roses (DRs) in black; MultiPods (MPs) in blue; NanoFlakes (NFs) in red; NanoCrystals (NCs) in green.

Table 1. Effect of ZnO particle types (control; MultiPods, MPs; NanoCrystals, NCs; NanoFlakes, NFs; Desert Roses, DRs), dosages (0, 12.5, 25.0, 50.0 mg L^{-1}), photoperiod (0/24; 24/24 day/night), and their interactions on the final germination percentage (FGP, %), radicle length (cm), and index of germination (IGe, %) of *Ocimum basilicum* seeds in the growth chamber assay.

Type (A)	FGP	Radicle Length	IGe
Control	52.2 b	5.25	100.0 b
MPs	65.4 ab	4.66	119.6 ab
NCs	71.1 a	4.39	122.5 ab
NFs	65.6 ab	4.54	119.4 ab
DRs	69.4 a	5.07	141.4 a
p	*	ns	**
Dosage (B)			
0	52.2 b	5.25 ab	100.0
12.5	65.4 a	5.35 a	138.3
25.0	69.2 a	4.72 ab	131.8
50.0	68.3 a	3.86 b	107.1
p	*	*	ns

Table 1. *Cont.*

Photoperiod (C)			
0/24	62.6	4.0	88.7
24/24	69.5	5.5	159.7
p	*	***	***
Interaction		*p*	
A × B	ns	ns	ns
A × C	ns	ns	ns
B × C	ns	ns	ns
A × B × C	ns	ns	ns

Mean values showing the same letter were not statistically different at $p < 0.05$. The statistical relevance is provided (* $p < 0.05$; ** $p < 0.01$; *** $p < 0.001$; ns = not significant).

Table 2. Effect of the applied photoperiods (0/24; 24/24 day/night) on the final germination percentage (FGP, %) and radicle length (cm) of control treatments in *Ocimum basilicum*, *Lactuca sativa*, and *Lepidium sativum* seeds in the growth chamber assay.

	O. basilicum		***L. sativa***		***L. sativum***	
Photoperiod	**FGP**	**Radicle Length**	**FGP**	**Radicle Length**	**FGP**	**Radicle Length**
0 h/24 h	53.3	5.43	30.0	2.43	95.0	35.21
24 h/24 h	50.0	4.88	23.3	1.55	100.0	26.82
p	ns	ns	ns	ns	ns	*

The statistical relevance is provided (* $p < 0.05$; ns = not significant).

The final germination percentage and the radicle length of *L. sativa* were not affected by the different ZnO particle types (Table 3). Regarding IGe, DRs resulted in higher values than NCs (113.5% and 62.1%, respectively). Regarding dosage, FGP was significantly reduced by the application of the highest concentration (50.0 mg L^{-1}) in comparison to the control and 12.5 mg L^{-1} (17.5, 27.7, and 30.0%, respectively). No effect on radicle length and IGe was observed. As for *O. basilicum*, no effect of the photoperiod was highlighted in control conditions (Table 2). Thus, 24 h of light severely declined all the traits, reducing FGP by ~−70%, radicle length by ~−50%, and IGe by ~−50% with respect to dark conditions.

Table 3. Effect of ZnO particle types (control; MultiPods, MPs; NanoCrystals, NCs; NanoFlakes, NFs; Desert Roses, DRs), dosages (0, 12.5, 25.0, 50.0 mg L^{-1}), photoperiods (0/24; 24/24 day/night), and their interactions on the final germination percentage (FGP, %), radicle length (cm), and index of germination (IGe, %) of *Lactuca sativa* seeds in the growth chamber assay.

Type (A)	**FGP**	**Radicle Length**	**IGe**
Control	27.8	2.14	100.0 ab
MPs	25.0	2.21	105.3 ab
NCs	20.0	1.59	62.1 b
NFs	21.7	1.69	75.5 ab
DRs	28.3	1.93	113.5 a
p	ns	ns	*
Dosage (B)			
0	27.7 a	2.14	100.0
12.5	30.0 a	2.06	108.1
25.0	23.8 ab	1.60	82.3
50.0	17.5 b	1.90	78.3
p	**	ns	ns

Table 3. *Cont.*

Photoperiod (C)			
0/24	36.7	2.44	121.3
24/24	10.7	1.29	57.8
p	***	***	***
Interaction		*p*	
A × B	ns	ns	ns
A × C	*	ns	ns
B × C	ns	ns	ns
A × B × C	ns	ns	ns

Mean values showing the same letter were not statistically different at $p < 0.05$. The statistical relevance is provided (* $p < 0.05$; ** $p < 0.01$; *** $p < 0.001$; ns = not significant).

Regarding statistical interaction, a significant effect between ZnO particle type and photoperiod was found only for FGP (Table 4). The computed ANOVA highlighted the effect of DRs in dark conditions on increasing the FGP in comparison to all the tested particles and the control applied in 24 h of light.

Table 4. Effect of ZnO particle types (control; MultiPods, MPs; NanoCrystals, NCs; NanoFlakes, NFs; Desert Roses, DRs) and photoperiods (0/24; 24/24 day/night) on the final germination percentage (FGP, %) of *Lactuca sativa* seeds in the growth chamber assay.

Treatment	**FGP**
Control—0 h/24 h	30.0 ab
MPs—0 h/24 h	34.4 ab
NCs—0 h/24 h	33.3 ab
NFs—0 h/24 h	34.4 ab
DRs—0 h/24 h	48.8 a
Control—24 h/24 h	23.3 bc
MPs—24 h/24 h	15.5 bc
NCs—24 h/24 h	6.7 c
NFs—24 h/24 h	8.8 c
DRs—24 h/24 h	7.7 c
p	***

Mean values showing the same letter were not statistically different at $p < 0.05$. The statistical relevance is provided (*** $p < 0.001$).

The final germination percentage of *L. sativum* was not affected by all the tested ZnO particles, their dosage, or the applied photoperiods (Table 5), while the application of all particles significantly reduced radicle length in comparison to the control. As a significant reduction in radicle length was observed between control treatments in light conditions (Table 2), no further statistical analysis on photoperiod was conducted. Regarding IGe, all the treated particle types and dosages resulted in a significant reduction in this parameter, with the exception of DRs and the concentration of 50 mg L^{-1}.

Significant interactions among the effects of NP types and dosages were found for radicle length, indicating a reduction in this parameter due to the application of all the tested particles in comparison to the control.

3.3. The role of ZnO Particles in ROS Production

The detection of the generated ROS was performed under similar light irradiation conditions to those used for seed germination tests on the different water suspensions of ZnO particles. The same ROS generation was analyzed in dark conditions as a comparison (Figure 4). In particular, the hydroxyl radical (·OH) species was monitored by adopting the spin-trap technique exploiting the DMPO molecule. As can be clearly observed by the spectra recorded in the dark (Figure 4A), no ZnO particle was able to generate ROS in these

conditions, similar to what happened to the pure water sample. Under the light irradiation conditions used for seed germination, peaks related to the DMPO-OH spin adduct were clearly detected for the two microparticles, i.e., DRs and MPs, and the nanoparticle sample NCs, with a statistical significance (*** $p < 0.001$) between these samples and the pure water one and with respect to the samples in dark conditions. In particular, the ZnO DRs produced the highest amount of hydroxyl radicals (Figure 4C), with a molar concentration of the DMPO-OH adduct in solution equal to 2.7×10^{-5} M, statistically higher (* $p < 0.05$) than the one recorded for the NC (2×10^{-5} M) and MP (9.7×10^{-6} M, *** $p < 0.001$) samples. There was also statistical significance between the DMPO-OH concentration values related to the MP and NC samples (** $p < 0.01$).

Table 5. Effect of ZnO NP type (water; MultiPods, MPs; NanoCrystals, NCs; NanoFlakes, NFs; Desert Roses, DRs), dosage (0, 12.5, 25.0, 50.0 mg L^{-1}), photoperiod (0/24; 24/24 day/night), and their interactions on the final germination percentage (FGP, %), radicle length (cm), and index of germination (IGe, %) of *Lepidium sativum* seeds in the growth chamber assay.

Type (A)	FGP	Radicle Length	IGe
Control	96.7	32.4 a	100.0 a
MPs	97.2	26.9 b	86.6 b
NCs	95.0	25.1 b	79.3 b
NFs	92.2	24.1 b	73.4 b
DRs	93.9	27.9 b	87.3 ab
p	ns	*	*
Dosage (B)			
0	96.7	32.4 a	100.0 a
12.5	95.0	24.6 b	77.1 b
25.0	93.3	25.3 b	78.4 b
50.0	94.4	28.3 b	89.5 ab
p	ns	*	*
Photoperiod (C)			
0/24	94.5	-	-
24/24	95.1	-	-
p	ns		
Interaction		*p*	
A × B	ns	*	ns
A × C	ns	-	-
B × C	ns	-	-
A × B × C	ns	-	-

Mean values showing the same letter were not statistically different at $p < 0.05$. The statistical relevance is provided (* $p < 0.05$; ns = not significant). "-" means no data are available.

In contrast, no ROS were detected from the NF sample, confirming once again the low capability of this specific morphology to be photoexcited.

3.4. The Dissolution of ZnO Particles in Water

The dissolution tests in water were carried out for all four ZnO morphologies. The obtained values related to zinc cation detection in water revealed a complete dissolution of the four ZnO samples (Table 6). Starting from the number of ZnO particles dispersed in water, almost the same amount of zinc cations could be found in the solution after 72 h.

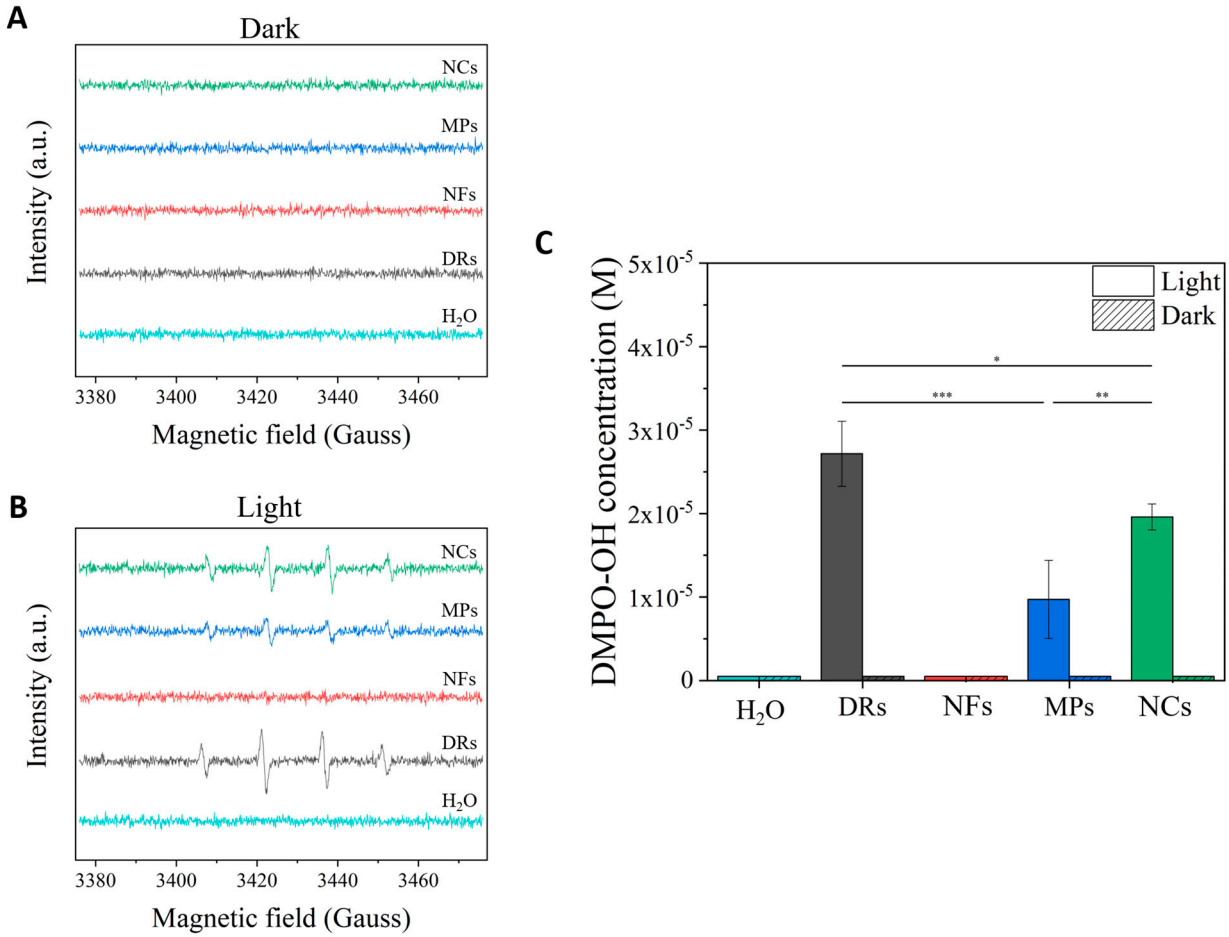

Figure 4. EPR (Electron Paramagnetic Resonance) spectra obtained by exposing the different ZnO particles to (**A**) dark and (**B**) light irradiation conditions (395 W m^{-2} for 10 min of white light). Spectra were recorded adopting the spin-trap technique and using the DMPO trap; thus, DMPO-OH adduct signals derived from the production of OH radicals were mainly recorded. (**C**) Bar graph comparing the DMPO-OH concentrations obtained from the different ZnO particles excited under light irradiation or dark. The statistical relevance is provided (* $p < 0.05$; ** $p < 0.01$; *** $p < 0.001$).

Table 6. Results of the water dissolution experiment after storing the different ZnO particles in water at RT, pH 7, for 72 h in the dark.

Sample	Nominal Starting Particle Concentration (mg L^{-1})	Obtained Zn Concentration (mg L^{-1})
ZnO DRs	12.5	12.8 ± 0.4
	25.0	25.1 ± 1.4
	50.0	49.1 ± 4.6
ZnO MPs	12.5	13.5 ± 1.3
	25.0	28.3 ± 2.2
	50.0	49.2 ± 3.3
ZnO NFs	12.5	13.9 ± 0.4
	25.0	24.9 ± 0.7
	50.0	50.5 ± 0.3
ZnO NCs	12.5	13.8 ± 0.9
	25.0	24.7 ± 1.0
	50.0	54.5 ± 5.1

4. Discussion

Nanoparticles are found to be very toxic to different plant species [46], while they play a crucial role in promoting plant growth in others [47,48]. Zinc is known to be involved in controlling enzymes, protein synthesis, cell elongation, regulating membrane function, and increasing plant tolerance to environmental stress [49], and high Zn content in seeds could act as a seed germination starter and promote early seedling growth by speeding up metabolism [50–52]. Muhammad et al. [53] demonstrated that ZnO nanoparticle priming increased Zn content in maize seed embryo tissues and aleurone layers. However, while the literature reports that ZnO in relatively low concentrations improved germination and seedling growth, while high concentrations of these nanoparticles showed toxic effects on seedlings [54], as also confirmed in this study, sensitivity to ZnO nanoparticles varies greatly from species to species.

In the present work, wide variability in the response to the type and concentration of ZnO micro- and nanoparticles and to the applied photoperiod was observed in the three different studied species. *O. basilicum* increased in FGP, particularly when treated with NPs and DRs at the lowest concentration (12.5 mg L^{-1}), and especially in light conditions (see Tables 1 and 2). At higher concentrations (50.0 mg L^{-1}), phytotoxicity in root development was observed. On the contrary, in *L. sativum*, a phytotoxic effect was seen on radicle length with all the used ZnO particles and concentrations (Table 5). *L. sativa*, however, did not show significant effects due to the type of particles, with a reduction in FGP only at higher concentrations (50.0 mg L^{-1}) and particularly in light conditions (see Tables 3 and 4). This is in contradiction with Lin and Jing [34] who, even with 2000 mg L^{-1} of Zn particles, did not report a negative effect on *L. sativa* seed germination. Within the range of the applied concentration in the present study, the data in the literature are not unique. The germination rate of *Lolium perenne* L. and *Zea mays* L. was decreased by up to 50%, even at concentrations ranging from 20 to 50 mg L^{-1} [34]. Similar behavior was measured also in *Brassica oleracea* var. *capitata* and *Brassica oleracea* var. *botrytis* [54]. On the other hand, increases in FGP and rootlet growth were highlighted in *Brassica napus* and *Camelina* seeds treated with 10 mg L^{-1}. Seed germination rates were unaffected in *Cucubita pepo* L. and Chinese cabbage [55] by four nano-ZnOs at concentrations ranging between 1 and 80 mg L^{-1}.

Considering these findings, several significant aspects arise, particularly concerning the initial stages of germination, rather than the subsequent development of the roots. In fact, this last parameter is generally reduced if the used concentrations of ZnO particles are too high (equal to 50.0 mg L^{-1} in the present study, see Tables 1, 3 and 5). The radicles were in direct contact with the particles and thus were the first tissues to be exposed to excess concentrations. Indeed, the water dissolution tests (as in Table 6) reported a complete degradation of all the ZnO particles into zinc cations within 72 h, which can be potentially toxic above certain concentrations. This result reveals that ZnO-containing solutions, irrespective of the ZnO morphology, can release zinc cations after prolonged immersion in water, i.e., 72 h. This zinc cation release is also dependent on the starting particle concentration, which can, in turn, influence seed germination, as discussed below. It is clear that, as soon as the ZnO micro- and nanostructures are fully dissolved in zinc cations, the disappearance of the semiconductive structure of ZnO completely undermines the production of ROS under light exposure conditions.

In the literature, ZnO was reported to inhibit the root elongation of several species such as *Raphanus sativus* L., *Brassica rapa* L., *L. perenne*, *L. sativa*, *Z. mays*, *L. sativum*, and *Cucumis sativus* L., and toxicity was considered to be mainly due to a particle-dependent effect [34,56].

The seeds' morphology, their ability to absorb ZnO particles, and their susceptibility to the release of ROS by ZnO particles under light exposure conditions are therefore the fundamental aspects to be further explored. Thus, our results related to seed germination indicate that the seed coats of *O. basilicum* and *L. sativa* were able to absorb the solutions containing the ZnO particles, as the FGP appeared to be significantly influenced in comparison to the control treatment. This phenomenon can be attributed to the selective permeability

of seed coats. Previous studies indicated that engineered nanoparticles could penetrate an intact seed coat via the intercellular spaces (<10 µm; indeed, the ZnO particles studied in this work had smaller dimensions) in the parenchyma, which are filled with aqueous media, facilitating the transport of soluble nutrients as well as small particles to the embryo tissues and increasing seed water uptake [57–62]. On the contrary, seed coats with selective permeability and secrete seed mucilage (i.e., *L. sativum*) are considered to play a very important role in protecting the embryo from harmful external factors [34,61]. Within seeds, entered nanoparticles may interact with cytoplasm proteins or even organelles, leading to changes in metabolism and cellular signaling, which stimulates a cellular response like that occurring during oxidative signaling [63]. Thus, the increase in the seed germination percentage in *O. basilicum* could be attributed to the role of ZnO by inducing a range of biochemical changes in the seed, such as the breaking of dormancy, the hydrolysis or metabolization of inhibitors, imbibition, and enzyme activation [64]. Broadley et al. [65] also reported that Zn^{2+} as cations acts as a component in the metabolism of carbohydrates and proteins, resulting in the effective and synchronized germination of seeds primed with ZnO particles. On the contrary, the tested concentration resulted in phytotoxicity for *L. sativa* seeds.

ZnO particles with diverse morphologies, such as nanospheres, nanorods, and nanotubes, and sizes have been synthesized via various techniques [66]. However, the effects of the particle morphology and size of ZnO on seed germination and development remain unclear. Studies show that spherical nanoparticles with a 30 nm diameter significantly inhibit growth and germination parameters compared to larger nanoparticles (150 nm in diameter) [67]. As reported by Xiang et al. [67], in addition to the "dose-effect" relationship, nanotoxicity displays "size-dependent" and "morphology-dependent" tendencies. Here, for example, we analyzed different sizes and morphologies of ZnO from nano- to micro-sized particles, each of them also showing different surface areas, with the NCs and DRs having the highest surface area (61 and 16 m^2/g, respectively, as reported by Lops et al. [23] with respect to MPs and NFs (7 and 1 m^2/g, respectively [23])). In nanomedicine, the therapeutic effect of ZnO particles is accomplished by the release of harmful species (i.e., ROS) upon the interaction of ZnO with aqueous media and light [68,69]. Nanoparticles are reported to mediate the generation of ROS, which act as signaling molecules for storage organs to bring about the mobilization of reserve material and support rapid axis growth, which also results in the cell wall loosening and endosperm weakening of treated seeds [8]. In the present study, we reported three to four different ZnO micro- and nanoparticles (Figure 1) able to produce, upon light irradiation, different levels of ROS in water (Figure 4). In particular, the ZnO DR morphology produced the highest amount of DMPO-OH adduct (up to 2.7×10^{-5} M) due to the generation of ·OH radicals, followed by the ZnO NP morphology, producing up to 2.0×10^{-5} M. ROS produced by NPs and DRs are indeed potentially another crucial player in increasing the seed germination rate of *O. basilicum*, while they may induce an opposite action in *L. sativa*. In fact, as stated by Paul et al. [1], enhanced ROS during seed priming can be seen as a necessary evil for germination. Though ROS appear to be harmful to the cell, they are a pivotal determinant of seed germination priming as they activate downstream MAPKs, calcium-binding proteins, and calcium ion channels or inhibit protein phosphatases [70,71]. However, ROS have a dual function in seed germination since they facilitate germination and release dormancy at low concentrations, trigger cell death, and inhibit seed germination at higher concentrations [72]. But, as reported here, this phenomenon is strictly species-specific. These results clearly show that ZnO-containing water solutions used for seed germination are in principle able to generate ROS, except when adopting the NF morphology of ZnO. However, determining the level of ROS concentration is not univocal and strictly depends on the seed species. It is well known that ROS have a short life, in the range of picoseconds, and they can be generated as far as the ZnO semiconductor material is present and irradiated by light. Since ZnO has well-known chemical instability and is prone to dissolve into zinc cations (Zn^{2+}) in water solutions, we have examined the stability over time of the four ZnO micro- and

nanoparticles in water. Given the differences found in this work, the application of these nanoparticles in nanopriming must be evaluated based on the horticultural species to be treated. Thus, *O. basilicum* seed priming with ZnO nanoparticles could be an economical and environmentally friendly smart farming approach. The introduction of this smart farming practice may help in achieving the goal of the agri-seed industry in the future to enhance seed germination and improve overall crop yields.

5. Conclusions

The present study demonstrated that different plant species, a range of ZnO micro- and nanoparticle types and concentrations, and even light exposure differences in experimental conditions may bring about different or even completely opposite experimental results. The combined effect of light, Zn ions, and ROS concentration within seed coats appears to be species-dependent, thus resulting in a significant increase in seed germination and vigor in *O. basilicum* seeds treated with NCs and DRs at 25 ppm and a reduction in *L. sativa*, with no effect on *L. sativum*. Given that the higher ROS values were obtained by using the DR and NP types starting from a concentration between 100 and 200 times higher of ZnO particles than those tested on seeds, it can be hypothesized that a concentration ranging between 1.35×10^{-7} M and 2.7×10^{-7} M of DMPO-OH adduct may be a limit between the positive and negative ROS action during seed germination of the tested species. Positive or negative outcomes hinge on factors such as the type and dosage of nanomaterials, treatment methods, developmental stage, species genotype, and environmental conditions. Without a comprehensive understanding of the diverse interactions between ZnO NPs and the plant genome or epigenome, leveraging these resources for maximum benefit as replacements for conventional growth promoters or protectants remains challenging. Achieving this necessitates the establishment of suitable techniques to discern plant conditions and optimize nanomaterial treatments. Changes induced by the studied ZnO particles in the physiology and biochemistry of seeds may bring the induction of specific secondary metabolites. However, it is necessary to evaluate in more detail the effects of these particles to understand the specific molecular and biochemical changes they cause in seeds in future studies.

Supplementary Materials: The following supporting information can be downloaded at: https://www.mdpi.com/article/10.3390/horticulturae10060575/s1, Figure S1. Optical fluorescence microscopy images collected on ZnO desert roses (DRs). Figure S2. Optical fluorescence microscopy images collected on ZnO multipods (MPs). Figure S3. Optical fluorescence microscopy images collected on ZnO nanoflakes (NFs). Figure S4. Optical fluorescence microscopy images collected on ZnO nanocrystals (NCs).

Author Contributions: Conceptualization, M.C. and V.C.; Methodology, M.C., N.M.P. and V.C.; Validation, V.C.; Investigation, M.C., N.M.P. and V.C.; Resources, V.C.; Data curation, M.C., N.M.P. and V.C.; Writing—original draft, M.C.; Writing—review & editing, M.C., N.M.P. and V.C. All authors have read and agreed to the published version of the manuscript.

Funding: This research received no external funding.

Data Availability Statement: Data is contained within the article and Supplementary Materials.

Conflicts of Interest: The authors declare no conflict of interest.

References

1. Paul, S.; Dey, S.; Kundu, R. Seed priming: An emerging tool towards sustainable agriculture. *Plant Growth Regul.* **2022**, *97*, 215–234. [CrossRef]
2. Tanou, G.; Vasileios, F.; Athanassios, M. Priming against environmental challenges and proteomics in plants: Update and agricultural perspectives. *Front. Plant Sci.* **2012**, *3*, 31211. [CrossRef] [PubMed]
3. Butler, L.H.; Hay, F.R.; Ellis, R.H.; Smith, R.D.; Murray, T.B. Priming and re-drying improve the survival of mature seeds of *Digitalis purpurea* during storage. *Ann. Bot.* **2009**, *103*, 1261–1270. [CrossRef] [PubMed]
4. Paparella, S.; Araújo, S.S.; Rossi, G.; Wijayasinghe, M.A.L.A.K.A.; Carbonera, D.; Balestrazzi, A. Seed priming: State of the art and new perspectives. *Plant Cell Rep.* **2015**, *34*, 1281–1293. [CrossRef] [PubMed]

5. Farooq, M.; Basra, S.M.A.; Ahmad, N.; Hafeez, K. Thermal hardening: A new seed vigor enhancement tool in rice. *J. Integr. Plant Biol.* **2005**, *47*, 187–193. [CrossRef]
6. Araujo, S.D.S.; Paparella, S.; Dondi, D.; Bentivoglio, A.; Carbonera, D.; Balestrazzi, A. Physical methods for seed invigoration: Advantages and challenges in seed technology. *Front. Plant Sci.* **2016**, *7*, 194485. [CrossRef] [PubMed]
7. An, R.; Liang, Y.; Deng, R.; Lei, P.; Zhang, H. Hollow nanoparticles synthesized via Ostwald ripening and their upconversion luminescence-mediated Boltzmann thermometry over a wide temperature range. *Light Sci. Appl.* **2022**, *11*, 217. [CrossRef] [PubMed]
8. Mahakham, W.; Theerakulpisut, P.; Maensiri, S.; Phumying, S.; Sarmah, A.K. Environmentally benign synthesis of phytochemicals-capped gold nanoparticles as nanopriming agent for promoting maize seed germination. *Sci. Total Environ.* **2016**, *573*, 1089–1102. [CrossRef] [PubMed]
9. Pramanik, P.; Krishnan, P.; Maity, A.; Mridha, N.; Mukherjee, A.; Rai, V. Application of nanotechnology in agriculture. *Environ. Nanotechnol.* **2020**, *4*, 317–348.
10. Demasi, S.; Caser, M.; Caldera, F.; Dhakar, N.K.; Vidotto, F.; Trotta, F.; Scariot, V. Functionalized dextrin-based nanosponges as effective carriers for the herbicide ailanthone. *Ind. Crops Prod.* **2021**, *164*, 113346. [CrossRef]
11. Rai-Kalal, P.; Jajoo, A. Priming with zinc oxide nanoparticles improve germination and photosynthetic performance in wheat. *Plant Physiol. Biochem.* **2021**, *160*, 341–351. [CrossRef] [PubMed]
12. Mahakham, W.; Sarmah, A.K.; Maensiri, S.; Theerakulpisut, P. Nanopriming technology for enhancing germination and starch metabolism of aged rice seeds using phytosynthesized silver nanoparticles. *Sci. Rep.* **2017**, *7*, 8263. [CrossRef] [PubMed]
13. Zheng, M.; Tao, Y.; Hussain, S.; Jiang, Q.; Peng, S.; Huang, J.; Cui, K.; Nie, L. Seed priming in dry direct-seeded rice: Consequences for emergence, seedling growth and associated metabolic events under drought stress. *Plant Growth Regul.* **2016**, *78*, 167–178. [CrossRef]
14. Panyuta, O.; Belava, V.; Fomaidi, S.; Kalinichenko, O.; Volkogon, M.; Taran, N. The effect of pre-sowing seed treatment with metal nanoparticles on the formation of the defensive reaction of wheat seedlings infected with the eyespot causal agent. *Nanoscale Res. Lett.* **2016**, *11*, 92. [CrossRef] [PubMed]
15. Abdel Latef, A.A.H.; Abu Alhmad, M.F.; Abdelfattah, K.E. The possible roles of priming with ZnO nanoparticles in mitigation of salinity stress in lupine (*Lupinus termis*) plants. *J. Plant Growth Regul.* **2017**, *36*, 60–70. [CrossRef]
16. Mohamed, A.K.S.; Qayyum, M.F.; Abdel-Hadi, A.M.; Rehman, R.A.; Ali, S.; Rizwan, M. Interactive effect of salinity and silver nanoparticles on photosynthetic and biochemical parameters of wheat. *Arch. Agron. Soil Sci.* **2017**, *63*, 1736–1747. [CrossRef]
17. Govindaraju, K.; Anand, K.V.; Anbarasu, S.; Theerthagiri, J.; Revathy, S.; Krupakar, P.; Durai, G.; Kannan, M.; Subramanian, K.S. Seaweed (*Turbinaria ornata*)-assisted green synthesis of magnesium hydroxide [$Mg(OH)_2$] nanomaterials and their anti-mycobacterial activity. *Mater. Chem. Phys.* **2020**, *239*, 122007. [CrossRef]
18. Anand, K.V.; Anugraga, A.R.; Kannan, M.; Singaravelu, G.; Govindaraju, K. Bio-engineered magnesium oxide nanoparticles as nano-priming agent for enhancing seed germination and seedling vigour of green gram (*Vigna radiata* L.). *Mater. Lett.* **2020**, *271*, 127792. [CrossRef]
19. Kumar, D.; Patel, K.P.; Ramani, V.P.; Shukla, A.K.; Meena, R.S. Management of micronutrients in soil for the nutritional security. In *Nutrient Dynamics for Sustainable Crop Production*; Springer: Singapore, 2020; pp. 103–134.
20. Shelar, A.; Singh, A.V.; Maharjan, R.S.; Laux, P.; Luch, A.; Gemmati, D.; Tisato, V.; Singh, S.P.; Akanksha, S.; Manohar, C.; et al. Sustainable agriculture through multidisciplinary seed nanopriming: Prospects of opportunities and challenges. *Cells* **2021**, *10*, 2428. [CrossRef]
21. Cauda, V.; Gazia, R.; Porro, S.; Stassi, S.; Canavese, G.; Roppolo, I.; Chiolerio, A. Nanostructured ZnO materials: Synthesis, properties and applications. In *Handbook of Nanomaterials Properties*; Springer: Berlin/Heidelberg, Germany, 2014; pp. 137–177.
22. Rameshraddy, P.G.J.; Rajashekar, R.B.H.; Salimath, M.; Geetha, K.N.; Shankar, A.G. Zinc oxide nano particles increases Zn uptake, translocation in rice with positive effect on growth, yield and moisture stress tolerance. *Ind. J. Plant Physiol.* **2017**, *22*, 287–294. [CrossRef]
23. Lops, C.; Ancona, A.; Di Cesare, K.; Dumontel, B.; Garino, N.; Canavese, G.; Hérnandez, S.; Cauda, V. Sonophotocatalytic degradation mechanisms of Rhodamine B dye via radicals generation by micro-and nano-particles of ZnO. *Appl. Catal. B Environm.* **2019**, *243*, 629–640. [CrossRef]
24. Dumontel, B.; Canta, M.; Engelke, H.; Chiodoni, A.; Racca, L.; Ancona, A.; Limongi, T.; Canavese, G.; Cauda, V. Enhanced biostability and cellular uptake of zinc oxide nanocrystals shielded with a phospholipid bilayer. *J. Mater. Chem. B* **2017**, *5*, 8799–8813. [CrossRef] [PubMed]
25. Ancona, A.; Dumontel, B.; Garino, N.; Demarco, B.; Chatzitheodoridou, D.; Fazzini, W.; Engelke, H.; Cauda, V. Lipid-coated zinc oxide nanoparticles as innovative ROS-generators for photodynamic therapy in cancer cells. *Nanomaterials* **2018**, *8*, 143. [CrossRef]
26. Sosan, A.; Svistunenko, D.; Straltsova, D.; Tsiurkina, K.; Smolich, I.; Lawson, T.; Subramaniam, S.; Golovko, V.; Anderson, D.; Sokolik, A.; et al. Engineered silver nanoparticles are sensed at the plasma membrane and dramatically modify the physiology of *Arabidopsis thaliana* plants. *Plant J.* **2016**, *85*, 245–257. [CrossRef]
27. Balážová, Ľ.; Baláž, M.; Babula, P. Zinc oxide nanoparticles damage tobacco BY-2 cells by oxidative stress followed by processes of autophagy and programmed cell death. *Nanomaterials* **2020**, *10*, 1066. [CrossRef]
28. Peng, C.; Zhang, W.; Gao, H.; Li, Y.; Tong, X.; Li, K.; Zhu, X.; Wang, Y.; Chen, Y. Behavior and potential impacts of metal-based engineered nanoparticles in aquatic environments. *Nanomaterials* **2017**, *7*, 21. [CrossRef] [PubMed]

29. Auld, D.S. Zinc coordination sphere in biochemical zinc sites. In *Zinc Biochemistry, Physiology, and Homeostasis: Recent Insights and Current Trends*; Springer: Dordrecht, The Netherlands, 2001; pp. 85–127.
30. Toor, M.D.; Adnan, M.; Javed, M.S.; Habibah, U.; Arshad, A.; Din, M.M.; Ahmad, R. Foliar application of Zn: Best way to mitigate drought stress in plants; A review. *Int. J. Appl. Res.* **2020**, *6*, 16–20.
31. Estrada-Urbina, J.; Cruz-Alonso, A.; Santander-González, M.; Méndez-Albores, A.; Vázquez-Durán, A. Nanoscale zinc oxide particles for improving the physiological and sanitary quality of a Mexican landrace of red maize. *Nanomaterials* **2018**, *8*, 247. [CrossRef] [PubMed]
32. Mahajan, P.; Dhoke, S.K.; Khanna, A.S. Effect of nano-ZnO particle suspension on growth of mung (*Vigna radiata*) and gram (*Cicer arietinum*) seedlings using plant agar method. *J. Nanotechn.* **2011**, *2011*, 696535. [CrossRef]
33. Ma, H.; Williams, P.L.; Diamond, S.A. Ecotoxicity of manufactured ZnO nanoparticles—A review. *Environ. Pollut.* **2013**, *172*, 76–85. [CrossRef]
34. Lin, D.; Xing, B. Phytotoxicity of nanoparticles: Inhibition of seed germination and root growth. *Environ. Pollut.* **2007**, *150*, 243–250. [CrossRef] [PubMed]
35. Lin, D.; Xing, B. Root uptake and phytotoxicity of ZnO nanoparticles. *Environ. Sci. Technol.* **2008**, *42*, 5580–5585. [CrossRef] [PubMed]
36. Lee, S.; Chung, H.; Kim, S.; Lee, I. The genotoxic effect of ZnO and CuO nanoparticles on early growth of buckwheat, *Fagopyrum esculentum*. *Water Air Soil Pollut.* **2013**, *224*, 1688. [CrossRef]
37. Raja, K.; Sowmya, R.; Sudhagar, R.; Moorthy, P.S.; Govindaraju, K.; Subramanian, K.S. Biogenic ZnO and Cu nanoparticles to improve seed germination quality in blackgram (*Vigna mungo*). *Mater. Lett.* **2019**, *235*, 164–167. [CrossRef]
38. Kaur, R.; Chandra, J.; Keshavkant, S. Nanotechnology: An efficient approach for rejuvenation of aged seeds. *Physiol. Mol. Biol. Plants* **2021**, *27*, 399–415. [CrossRef] [PubMed]
39. Wang, X.P.; Li, Q.Q.; Pei, Z.M.; Wang, S.C. Effects of zinc oxide nanoparticles on the growth, photosynthetic traits, and antioxidative enzymes in tomato plants. *Biol. Plant.* **2018**, *62*, 801–808. [CrossRef]
40. Rastogi, A.; Zivcak, M.; Sytar, O.; Kalaji, H.M.; He, X.; Mbarki, S.; Brestic, M. Impact of metal and metal oxide nanoparticles on plant: A critical review. *Front. Chem.* **2017**, *5*, 78. [CrossRef] [PubMed]
41. Kataria, S.; Jain, M.; Rastogi, A.; Živčák, M.; Brestic, M.; Liu, S.; Tripathi, D.K. Role of nanoparticles on photosynthesis: Avenues and applications. In *Nanomaterials in Plants, Algae and Microorganisms*; Academic Press: Cambridge, MA, USA, 2019; pp. 103–127.
42. Garino, N.; Limongi, T.; Dumontel, B.; Canta, M.; Racca, L.; Laurenti, M.; Castellino, M.; Casu, A.; Falqui, A.; Cauda, V. A microwave-assisted synthesis of zinc oxide nanocrystals finely tuned for biological applications. *Nanomaterials* **2019**, *9*, 212. [CrossRef]
43. ISTA. *International Rules for Seed Testing 2014*; ISTA: Antalya, Turkey, 2013; ISSN 2310-3655. Available online: https://www.seedtest.org/en/services-header/tools.html (accessed on 19 January 2021).
44. Caser, M.; Demasi, S.; Caldera, F.; Dhakar, N.K.; Trotta, F.; Scariot, V. Activity of *Ailanthus altissima* (Mill.) swingle extract as a potential bioherbicide for sustainable weed management in horticulture. *Agronomy* **2020**, *10*, 965. [CrossRef]
45. Caser, M.; Demasi, S.; Mozzanini, E.; Chiavazza, P.M.; Scariot, V. Germination Performances of 14 Wildflowers screened for shaping urban landscapes in mountain areas. *Sustainability* **2022**, *14*, 2641. [CrossRef]
46. Khan, I.; Saeed, K.; Khan, I. Nanoparticles: Properties, applications and toxicities. *Arab. J. Chem.* **2019**, *12*, 908–931. [CrossRef]
47. Zhou, P.; Adeel, M.; Shakoor, N.; Guo, M.; Hao, Y.; Azeem, I.; Li, M.; Liu, M.; Rui, Y. Application of nanoparticles alleviates heavy metals stress and promotes plant growth: An overview. *Nanomaterials* **2020**, *11*, 26. [CrossRef]
48. Noman, M.; Shahid, M.; Ahmed, T.; Tahir, M.; Naqqash, T.; Muhammad, S.; Song, F.; Abid, H.M.A.; Aslam, Z. Green copper nanoparticles from a native *Klebsiella pneumoniae* strain alleviated oxidative stress impairment of wheat plants by reducing the chromium bioavailability and increasing the growth. *Ecotoxicol. Environ. Saf.* **2020**, *192*, 110303. [CrossRef]
49. Cakmak, I. Enrichment of cereal grains with zinc: Agronomic or genetic biofortification? *Plant Soil* **2008**, *302*, 1–17. [CrossRef]
50. Singh, N.B.; Amist, N.; Yadav, K.; Singh, D.; Pandey, J.K.; Singh, S.C. Zinc oxide nanoparticles as fertilizer for the germination, growth and metabolism of vegetable crops. *J. Nanoeng. Nanomanufacturing* **2013**, *3*, 353–364. [CrossRef]
51. Dimkpa, C.O.; White, J.C.; Elmer, W.H.; Gardea-Torresdey, J. Nanoparticle and ionic Zn promote nutrient loading of sorghum grain under low NPK fertilization. *J. Agric. Food Chem.* **2017**, *65*, 8552–8559. [CrossRef]
52. Rashid, M.H.; Rahman, M.M.; Halim, M.A.; Naidu, R. Growth, metal partitioning and antioxidant enzyme activities of mung beans as influenced by zinc oxide nanoparticles under cadmium stress. *Crop Pasture Sci.* **2022**, *73*, 862–876. [CrossRef]
53. Muhammad, I.; Kolla, M.; Volker, R.; Günter, N. Impact of nutrient seed priming on germination, seedling development, nutritional status and grain yield of maize. *J. Plant Nutr.* **2015**, *38*, 1803–1821. [CrossRef]
54. Sarkhosh, S.; Kahrizi, D.; Darvishi, E.; Tourang, M.; Haghighi-Mood, S.; Vahedi, P.; Ercisli, S. Research Article Effect of Zinc Oxide Nanoparticles (ZnO-NPs) on Seed Germination Characteristics in Two Brassicaceae Family Species: *Camelina sativa* and *Brassica napus* L. *J. Nanomater.* **2022**, *2022*, 1892759. [CrossRef]
55. Stampoulis, D.; Sinha, S.K.; White, J.C. Assay-dependent phytotoxicity of nanoparticles to plants. *Environ. Sci. Technol.* **2009**, *43*, 9473–9479. [CrossRef] [PubMed]
56. Manzo, S.; Rocco, A.; Carotenuto, R.; De Luca Picione, F.; Miglietta, M.L.; Rametta, G.; Di Francia, G. Investigation of ZnO nanoparticles' ecotoxicological effects towards different soil organisms. *Environ. Sci. Pollut. Res.* **2011**, *18*, 756–763. [CrossRef] [PubMed]

57. Lee, C.W.; Mahendra, S.; Zodrow, K.; Li, D.; Tsai, Y.C.; Braam, J.; Alvarez, P.J. Developmental phytotoxicity of metal oxide nanoparticles to *Arabidopsis thaliana*. *Environ. Toxicol. Chem. Int. J.* **2010**, *29*, 669–675. [CrossRef] [PubMed]
58. Van Dongen, J.T.; Ammerlaan, A.M.; Wouterlood, M.; Van Aelst, A.C.; Borstlap, A.C. Structure of the developing pea seed coat and the post-phloem transport pathway of nutrients. *Ann. Bot.* **2003**, *91*, 729–737. [CrossRef] [PubMed]
59. Wang, M.; Gao, B.; Tang, D. Review of key factors controlling engineered nanoparticle transport in porous media. *J. Hazard. Mater.* **2016**, *318*, 233–246. [CrossRef] [PubMed]
60. Eckhardt, S.; Brunetto, P.S.; Gagnon, J.; Priebe, M.; Giese, B.; Fromm, K.M. Nanobio silver: Its interactions with peptides and bacteria, and its uses in medicine. *Chem. Rev.* **2013**, *113*, 4708–4754. [CrossRef] [PubMed]
61. Kurepa, J.; Paunesku, T.; Vogt, S.; Arora, H.; Rabatic, B.M.; Lu, J.; Wanzer, M.B.; Woloschak, G.E.; Smalle, J.A. Uptake and distribution of ultrasmall anatase TiO_2 Alizarin red S nanoconjugates in *Arabidopsis thaliana*. *Nano Lett.* **2010**, *10*, 2296–2302. [CrossRef]
62. Qian, H.; Peng, X.; Han, X.; Ren, J.; Sun, L.; Fu, Z. Comparison of the toxicity of silver nanoparticles and silver ions on the growth of terrestrial plant model *Arabidopsis thaliana*. *J. Environ. Sci.* **2013**, *25*, 1947–1956.
63. Nile, S.H.; Thiruvengadam, M.; Wang, Y.; Samynathan, R.; Shariati, M.A.; Rebezov, M.; Nile, A.; Sun, M.; Venkidasamy, B.; Xiao, J.; et al. Nano-priming as emerging seed priming technology for sustainable agriculture—Recent developments and future perspectives. *J. Nanobiotechnol.* **2022**, *20*, 254. [CrossRef] [PubMed]
64. Harris, A.T.; Bali, R. On the formation and extent of uptake of silver nanoparticles by live plants. *J. Nanopart. Res.* **2008**, *10*, 691–695. [CrossRef]
65. Broadley, M.R.; White, P.J.; Hammond, J.P.; Zelko, I.; Lux, A. Zinc in plants. *New Phytol.* **2007**, *173*, 677–702. [CrossRef]
66. Zhai, T.; Xie, S.; Zhao, Y.; Sun, X.; Lu, X.; Yu, M.; Xu, M.; Xiao, F.; Tong, Y. Controllable synthesis of hierarchical ZnO nanodisks for highly photocatalytic activity. *CrystEngComm* **2012**, *14*, 1850–1855. [CrossRef]
67. Xiang, L.; Zhao, H.M.; Li, Y.W.; Huang, X.P.; Wu, X.L.; Zhai, T.; Yuan, Y.; Cai, Q.Y.; Mo, C.H. Effects of the size and morphology of zinc oxide nanoparticles on the germination of Chinese cabbage seeds. *Environ. Sci. Pollut. Res.* **2015**, *22*, 10452–10462. [CrossRef]
68. Vighetto, V.; Ancona, A.; Racca, L.; Limongi, T.; Troia, A.; Canavese, G.; Cauda, V. The synergistic effect of nanocrystals combined with ultrasound in the generation of reactive oxygen species for biomedical applications. *Front. Bioeng. Biotechnol.* **2019**, *7*, 374. [CrossRef]
69. Carofiglio, M.; Barui, S.; Cauda, V.; Laurenti, M. Doped zinc oxide nanoparticles: Synthesis, characterization and potential use in nanomedicine. *Appl. Sci.* **2020**, *10*, 5194. [CrossRef]
70. Diaz-Vivancos, P.; Barba-Espín, G.; Hernández, J.A. Elucidating hormonal/ROS networks during seed germination: Insights and perspectives. *Plant Cell Rep.* **2013**, *32*, 1491–1502. [CrossRef]
71. León-López, L.; Escobar-Zúñiga, Y.; Salazar-Salas, N.Y.; Mora Rochín, S.; Cuevas-Rodríguez, E.O.; Reyes-Moreno, C.; Milán-Carrillo, J. Improving polyphenolic compounds: Antioxidant activity in chickpea sprouts through elicitation with hydrogen peroxide. *Foods* **2020**, *9*, 1791. [CrossRef]
72. Jeevan Kumar, S.P.; Rajendra Prasad, S.; Banerjee, R.; Thammineni, C. Seed birth to death: Dual functions of reactive oxygen species in seed physiology. *Ann. Bot.* **2015**, *116*, 663–668. [CrossRef]